Journal of Power Sources 195 (2010) 509–515

Contents lists available at ScienceDirect

Journal of Power Sources

journal homepage: www.elsevier.com/locate/jpowsour

Electrical and thermal conductivities of novel metal mesh hybrid polymer composite bipolar plates for proton exchange membrane fuel cells

Min-Chien Hsiao[a], Shu-Hang Liao[a], Ming-Yu Yen[a], Chen-Chi M. Ma[a,*], Shuo-Jen Lee[b], Yung-Hung Chen[b], Chih-Hung Hung[c], Yu-Feng Lin[d], Xiao-Feng Xie[e]

[a] Department of Chemical Engineering, National Tsing Hua University, 101, Section 2 Kuang Fu Road, Hsin-Chu 30043, Taiwan, ROC
[b] Fuel Cell Center, Yuan Ze University, Tao-Yuan 32003, Taiwan, ROC
[c] Plastics Industry Development Center, Tai-Chung 40768, Taiwan, ROC
[d] Chemicals and Chemical Engineering, Chung Shan Institute of Science and Technology, Taoyuan 325, Taiwan, ROC
[e] Institute of Nuclear and New Energy technology, Tsinghua University, Beijing 100084, PR China

ARTICLE INFO

Article history:
Received 5 May 2009
Received in revised form 17 June 2009
Accepted 18 June 2009
Available online 26 June 2009

Keywords:
Fuel cell
Bipolar plate
Polymer composite
Metal mesh
Carbon nanotube

ABSTRACT

This study prepares novel metal mesh hybrid polymer composite bipolar plates for proton exchange membrane fuel cells (PEMFCs) via inserting a copper or aluminum mesh in polymer composites. The composition of polymer composites consists of 70 wt% graphite powder and 0–2 wt% modified multi-walled carbon nanotubes (m-MWCNTs). Results indicate that the in-plane electrical conductivity of m-MWCNTs/polymer composite bipolar plates increased from 156 S cm^{-1} (0 wt% MWCNT) to 643 S cm^{-1} (with 1 wt% MWCNT) (D.O.E. target >100 S cm^{-1}). The bulk thermal conductivities of the copper and aluminum mesh hybrid polymer composite bipolar plates (abbreviated to Cu-HPBP and Al-HPBP) increase from 27.2 W m^{-1} K^{-1} to 30.0 W m^{-1} K^{-1} and 30.4 W m^{-1} K^{-1}, respectively. The through-plane conductivities decrease from 37.8 S cm^{-1} to 36.7 S cm^{-1} for Cu-HPBP and 22.9 S cm^{-1} for Al-HPBP. Furthermore, the current and power densities of a single fuel cell using copper or aluminum mesh hybrid polymer composite bipolar plates are more stable than that of using neat polymer composite bipolar plates, especially in the ohmic overpotential region of the polarization curves of single fuel cell tests. The overall performance confirms that the metal mesh hybrid polymer composite bipolar plates prepared in this study are promising for PEMFC application.

1. Introduction

Proton exchange electrolyte membrane fuel cells (PEMFCs) exhibit the most promising alternative source of energy for a variety of portable electronic devices, stationary and vehicle applications [1–3]. To generate useful currents and voltages, individual single fuel cells are connected in series to form cell stacks. Thus, as one of the key components of PEMFCs, bipolar plates must exhibit excellent electrical conductivity as a current collector and adequate mechanical strength to resist clamping force during stack assembly. Traditionally, the machined graphite plate is the most used material for the bipolar plate due to its excellent corrosion resistance, low bulk density and high electrical conductivity [4–6]. However, the brittleness and high cost, difficulty in machining the flow channels on graphite plate [7] often limit using thin bipolar plates for reducing stack weight [6,8].

Previous researches have developed and investigated numerous alternative materials to reduce the cost and weight of the bipolar plate. Metallic materials such as stainless steel, aluminum, titanium and alloy or a protective coating layer on metallic plate surfaces have been widely investigated [9–11]. Metallic plates typically possess high bulk electrical conductivity, good thermal conductivity, and excellent mechanical properties [8,12]. However, several disadvantages are associated with metallic materials, including high density and possible leaching of metal ions into the membrane electrode assembly (MEA) [7,8]. Furthermore, any corrosion layer will lower the electrical conductivity of bipolar plates, and increase potential output loss due to high electrical resistance. Therefore, the requirements for bipolar plates in PEMFC include:

(1) high electrical conductivity (>100 S cm^{-1}) [13];
(2) good flexural strength (>25 MPa) [13];
(3) high impact strength (>40.5 J m^{-1}) [14];
(4) good chemical stability and corrosion resistance under PEMFC operating conditions (<10^{-6} A cm^{-2}) [15];
(5) high thermal conductivity to achieve stack cooling (>10 W m^{-1} K^{-1}) [14];

* Corresponding author. Tel.: +886 3571 3058; fax: +886 3571 5408.
E-mail addresses: ccma@che.nthu.edu.tw, d937603@oz.nthu.edu.tw, d9532814@oz.nthu.edu.tw (C.-C.M. Ma).

0378-7753/$ – see front matter © 2009 Published by Elsevier B.V.
doi:10.1016/j.jpowsour.2009.06.065

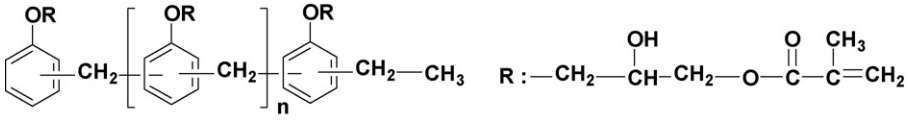

Scheme 1. Chemical structure of phenolic-novolac vinyl ester [17].

(6) low weight, especially for transportation; and
(7) low cost.

To replace graphite bipolar plates, graphite-based polymer composite bipolar plates are made from a combination of graphite, carbon powder filler or various fibers and polymer resin. Compared to graphite bipolar plates, polymer composites offer the advantages of lower cost, higher flexibility, and good processability. Gas flow channels can also be molded directly on the plate, eliminating the need for further machining [16,17]. High loading of carbon or graphite fillers must be incorporated into the composite bipolar plate to meet the minimum electrical conductivity required. However, high filler loading may cause a substantial reduction in strength and ductility of the composite bipolar plate, resulting in difficulty in making thin plates associated with high stack power densities [2,18,19]. Therefore, many literatures have reported several reinforced composite bipolar plates, including carbon–carbon composites [20], conventional conducting fillers/polymer matrix [8,21–23], thermosetting or thermoplastic polymer blending with multi-walled carbon nanotubes (MWCNTs) for use in composite materials [1,3,18,24–27]. Polymer composites incorporated with chemical modified CNTs (m-CNTs) possess excellent electrical conductivity and mechanical properties. When m-CNTs form infinite three-dimensional networks of connected paths through the insulating polymer matrix [28], CNTs may be suitable materials for composite bipolar plates.

At present, metallic bipolar plates and polymer composite bipolar plates have been developed individually. To maintain the advantages of metallic bipolar plates, some of their major disadvantages need improving. Kitta et al. [29] recently coated the stainless steel plate separator with corrosion-resistant and electronically conductive carbon/resin composite layers, followed by rib formation of a similar composite on the thin layers as gas flow fields. However, the coated composite film has very low electrical conductivity, only about 53 S cm^{-1} (less than the D.O.E. target >100 S cm^{-1}), and needs multi-step fabrication.

The current work introduces copper and aluminum mesh into polymer composite bipolar plates successfully developed in our previous researches [1,3,17]. This research investigates and compares through-plane conductivity, thermal conductivity and single fuel cell performance of these two types of bipolar plates.

2. Experimental

2.1. Materials

MWCNTs (trade name: C_{tube} 100) with a purity of 95% and a surface area of 150–250 m^2 g^{-1} were obtained from the CNT Co., Ltd., Korea. The diameters of MWCNTs are 10–50 nm and the lengths are 1–25 μm. Poly(oxyalkylene)-diamines (POA) were purchased from the Huntsman Chemical Co., Philadelphia, PA, USA, including poly(oxypropylene) (POP)-backboned diamines with the molecular weight of 2000 g mol^{-1}. Maleic anhydride (MA) was obtained from Showa Chemical Co., Gyoda City, Saotama, Japan. The phenolic-novolac epoxy-based vinyl ester (VE), was provided by the Swancor Co., Taiwan. Scheme 1 shows the chemical structure of the phenolic-novolac vinyl ester. Graphite powder was obtained from the Great Carbon Co., Ltd., Taiwan. The density of the graphite power was 1.88 g cm^{-3} and the particle size was less than 1000 μm. Metal mesh was obtained from Shang Kai Steel Co., Ltd., Taiwan. The short wide dimension (SWD) × long wide dimension (LWD) of alumina mesh is 1.5 mm × 3 mm, of copper mesh is 2 mm × 3.5 mm, the strand wide is 0.3 mm, the thickness is 0.2 mm, and the usage area is 2.5 cm × 2.5 cm.

2.2. Preparation of chemical modified MWCNTs

The oxidized MWCNTs (MWCNTs-COOH) were first prepared according to the HNO_3 treatment [1]. After this procedure, the functionalized MWCNTs (MWCNTs-COCl) with carbonyl chloride groups were prepared via the reaction of thionyl chloride with carboxyl-contained MWNT (MWNT-COOH) [30–32]. Finally, poly(oxyalkylene)-diamines (POA)–maleic anhydride (MA), abbreviated as POAMA (each POA bearing one MA, details of the preparation was illustrated in our previous paper [17]), molecules were introduced onto the surface of MWCNTs by the reaction of MWCNTs-COCl with amine group. The chemical modified MWCNTs with POAMA were denoted as MWCNTs–POAMA.

2.3. Preparation of bulk-molding compound (BMC) material and fabrication with/without metal mesh polymer composite bipolar plates

By using BMC method, polymer composite bipolar plates have been successfully developed by our group [16]. The BMC material was prepared by mixing the MWCNTs–POAMA/VE mixtures, low profile agent (polystyrene/styrene monomer (PS/SM) series), styrene monomer, thickening agent (MgO), release agent (Zinc Stearate, ZnSt), initiator (t-butyl peroxybenzoate, TBPB) and graphite in a kneader for 30 min. The BMC formulation is summarized in Table 1 [17]. After thickening for 36 h, the BMC was compression molded for 5 min at 140 °C.

The fabrications of metal mesh hybrid polymer composite bipolar plates are almost the same as above except a piece of aluminum mesh or copper mesh was inserted during hot-press.

2.4. Characterization and instruments

The in-plane electrical conductivity of the composite bipolar plate was examined with a four point probe detector (C4S-54/5S, Cascade Microtech, Beaverton, OR, USA). Thermal conductivity of bipolar plates is determined by a Hot Disk analyzer (TPS 2500,

Table 1
Formulation of BMC process [17].

Components	Composition	
	Resin composition (wt%)	BMC composition (wt%)
Vinyl ester	75	30
Low profile agent	8	
Styrene monomer	17	
TBPB	1.8	
Zinc stearate	3.5	
Magnesium oxide	1.8	
MWCNTs	0–2	
Graphite powder		70
Total		100

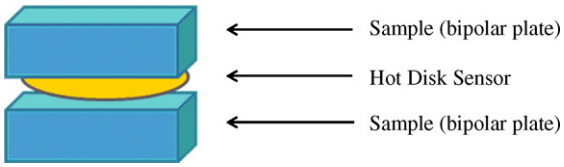

Scheme 2. Schematic of samples and sensor.

Sweden). Recently, the hot disk technique [33], which is a transient plane source technique (TPS) [34–38], has gained popularity as a tool for rapid and accurate thermal conductivity measurement (more detailed of the derivation was given by Ref. [33]). Scheme 2 shows the sensor is positioned between two pieces of bipolar plates.

To measure the through-plane conductivity [17], the composite bipolar plate sample with 30 mm × 30 mm and a thickness of 3 mm was placed between gold plated copper plates. Between the electrodes and sample was placed a piece of carbon paper (Toray TGP-H-120) to improve electrical contact between the electrodes and sample. The system was placed under an applied pressure of approximately 250 psi and the resistance was measured. The sample was removed, and the resistance of the test cell (including carbon paper) was measured again with the same conditions to obtain a "baseline" resistance. The sample resistance could then be calculated by subtracting the baseline resistance from the total resistance. The resistivity or conductivity of the sample was calculated by:

$$\rho = \frac{(R_T - R_{baseline})A}{L} \quad (1)$$

$$\sigma = \frac{1}{\rho} \quad (2)$$

where ρ is the resistivity, A is the contact area of sample, L is the thickness of sample, and R_T and $R_{baseline}$ are the total resistance and baseline resistance, respectively. The through-plane conductivity, σ, is defined as $1/\rho$.

A single PEMFC was developed at our laboratory as reported in previous paper [39]. The catalyst ink for the electrodes was prepared by mixing the catalyst powder (20 wt% Pt/C, E-TEK), Nafion® solution, and isopropyl alcohol. Then the prepared catalyst ink was sprayed on the wet-proof carbon paper with a platinum loading of 0.4 mg cm^{-2} for the anode and cathode. The membrane electrode assembly (MEA) was fabricated by placing the electrodes at both sides of pre-treated Nafion® 115 membrane, followed by hot pressing at 140 °C and 200 kg cm^{-2} for 90 s. The active electrode area was 4 cm^2. A single fuel cell was constructed from the prepared MEA, Teflon® gasket, and the prepared composite bipolar plate on both sides of the MEA. The thickness of the composite bipolar plates was 1.2 mm. The operating temperature and pressure of the single fuel cell were 70 °C and 1 atm, respectively. Hydrogen and oxygen gases were fed to the anode and cathode, respectively, after passing through a bubble humidifier, the flow rate ratio of the fuel and the oxidant was 1/1 (L min^{-1}). The performance of the single fuel cell was evaluated by measuring the *I–V* characteristics using an electronic load (Agilent, N3301A).

3. Results and discussion

3.1. The dispersion of pristine MWCNTs and MWCNTs–POAMA in vinyl ester matrix

Pristine carbon nanotubes (p-CNTs) have been used as lightweight high-strength fiber-reinforced nanomaterials in polymer composites due to their unique properties. However, owing to intrinsic Van der Waals forces, when mixed with polymer matrix, CNTs typically hold together as bundles or as entangled agglomerates and form heterogeneous regions. Chemical functionalization [1,3,17,31,39] of CNTs is one of the most common methods to obtain better dispersion. Fig. 1 shows MWCNT dispersion in vinyl ester matrix before (left) and after (right) chemical modification. Good MWCNT dispersion in the matrix is an important task when fabricating polymer composite bipolar plates, providing bipolar plates with improved mechanical strength, electrical conductivity, thermal stability, and most importantly improving single cell performances [1,3,17].

Fig. 1. Dispersion of p-MWCNTs (left) and MWCNTs–POAMA (right) in vinyl ester matrix.

3.2. The electrical conductivity of MWCNTs–POAMA/vinyl ester composite bipolar plates

Fig. 2 presents in-plane electrical conductivity of MWCNTs reinforced polymer composite bipolar plate as a function of MWCNT content. The figure shows that in-plane electrical conductivity in these two systems increases with MWCNT content, and dramatically increases at the percolation threshold [27,28] (around 0.25–0.5 wt%). The percolation threshold value essentially relates to MWCNT networking structures within the polymer, depending on MWCNT content. When the MWCNT-to-polymer ratio exceeds this value, in-plane electrical conductivity increases dramatically, due to the formation of MWCNT conduction network. However, poor dispersion of pristine MWCNT forms local cluster aggregation. This fact tends to increase the insulated polymer matrix region between MWCNTs. Higher in-plane electrical conductivity of MWCNTs–POAMA owes to better MWCNT dispersion in the vinyl ester matrix due to the grafting POAMA long chains on MWCNT. The individual MWCNTs–POAMA is easier to contact

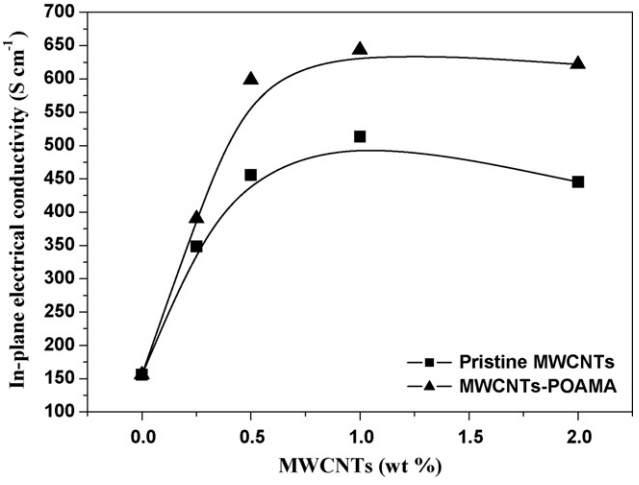

Fig. 2. The in-plane electrical conductivities of polymer composite bipolar plates with various MWCNTs.

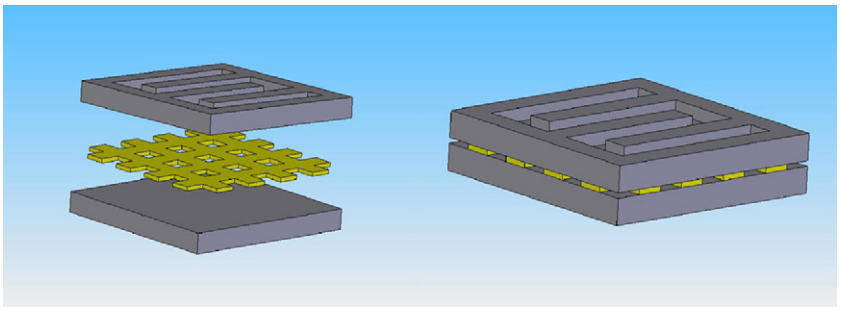

Fig. 3. Schematic of the structure of metal mesh hybrid polymer composite bipolar plates.

with each other. Consequently, with the same MWCNT content, the MWCNTs–POAMA/vinyl ester system possesses much higher electrical conductivity. Therefore, the grafting long chain POAMA on the MWCNTs surface not only results in better polymer matrix dispersion, but also efficiently enhances the electrical conductivity path.

Fig. 3 shows the fabrication scheme for the aluminum/copper metal mesh hybrid polymer composite bipolar plates. To obtain optimal electrical conductivity for hybrid bipolar plates, the present study uses 1 wt% MWCNTs–POAMA, and the in-plane electrical conductivity is 643 S cm^{-1}, much higher than the D.O.E. target (>100 S cm^{-1}).

3.3. Thermal conductivity of metal mesh–MWCNTs–POAMA/vinyl ester composite bipolar plates

Fig. 4 shows the fabricated product, denoted as Cu-HPBP (copper mesh hybrid polymer composite bipolar plate) and Al-HPBP (aluminum mesh hybrid polymer composite bipolar plates), respectively. Fig. 4(a) shows that flow channels can be molded directly on the plate, with a resulting thickness of 1.35 mm. In Fig. 4(c), the side view of the cross section of metal mesh bipolar plate also indicates that metal mesh can be completely imbedded in the original polymer composite bipolar plate.

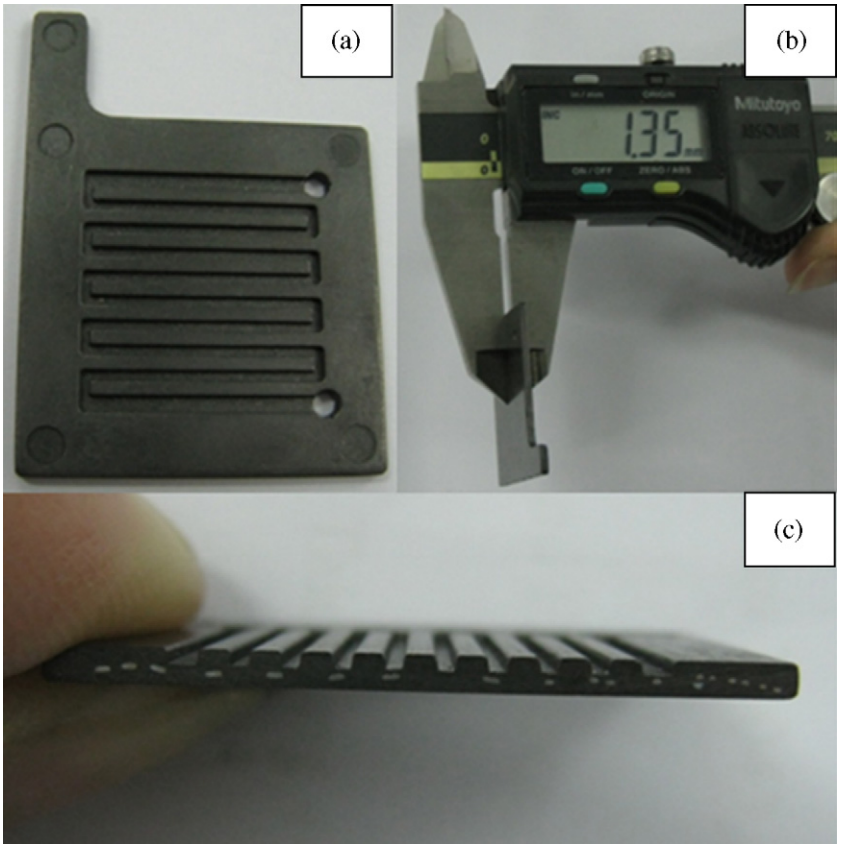

Fig. 4. The fabricated metal mesh polymer composite bipolar plate: (a) top view (reaction area is 2 cm × 2 cm), (b) the thickness (1.35 mm) and (c) the side view of the cross section.

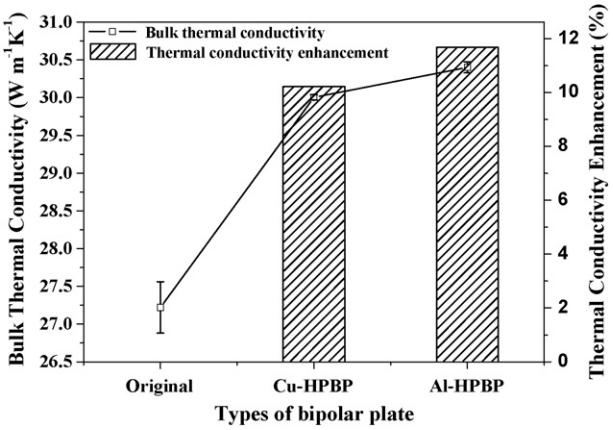

Fig. 5. The bulk thermal conductivity and thermal conductivity enhancement of original polymer composite, Cu-HPBP, and Al-HPBP with 1 wt% MWCNT loading.

Fig. 5 shows the bulk thermal conductivity (κ) and thermal conductivity enhancement (%) of the original polymer composite bipolar plate, Cu-HPBP, and Al-HPBP with 1 wt% MWCNT measured by the hot disk transient plane source method. The bipolar plates prepared with different metal meshes show the bulk thermal conductivities of $\kappa_{original} = 27.2\ W\ m^{-1}\ K^{-1}$ for the original polymer composite bipolar plate; $\kappa_{Cu\text{-}HPBP} = 30.0\ W\ m^{-1}\ K^{-1}$ for Cu-HPBP, and $\kappa_{Al\text{-}HPBP} = 30.4\ W\ m^{-1}\ K^{-1}$ for Al-HPBP. Thermal conductivity enhancements of Cu-HPBP and Al-HPBP are 10.2% and 11.7%, respectively. The metal mesh hybrid bipolar plate exhibits a synergistic effect on enhanced thermal conductivity and surpasses the original polymer composite bipolar plate. Faghri and Guo [40] have reported the commonly used cooling methods: (1) cooling with cathode oxidant flow, (2) cooling with separate air flow, (3) cooling with heat spreaders, and (4) water cooling. The metal meshes are intrinsically lightweight with high thermal conductivity; hence this research considers that metal meshes embedded in a polymer composite bipolar plate play a role of interior spreader for heat. This unique design not only dissipates heat accommodated in bipolar plates from the internal part more efficiently, but also implies that the reaction area temperature is more uniform due to proton exchange membrane vulnerability to burn at elevated temperatures. Waste heat must then be dissipated efficiently from the fuel cell to prevent hot spot formation on the membrane electrode assembly (MEA) and to protect the proton exchange membrane.

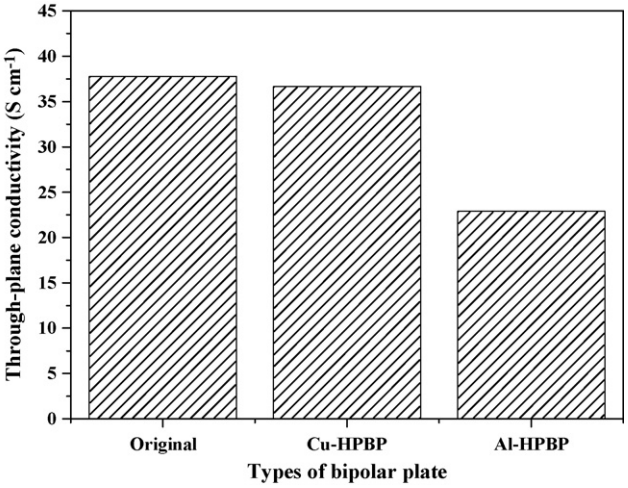

Fig. 6. The through-plane conductivity of original polymer composite, Cu-HPBP, and Al-HPBP with 1 wt% MWCNT loading.

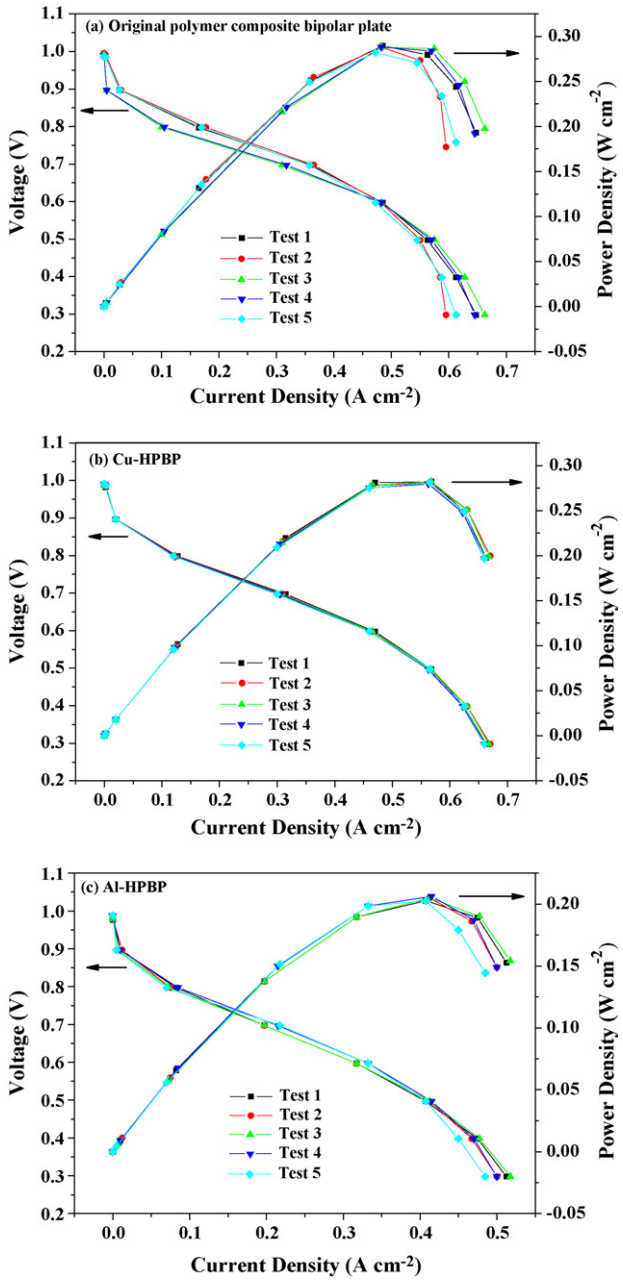

Fig. 7. Performance of the single cells assembled with (a) original polymer composite bipolar plate, (b) Cu-HPBP, and (c) Al-HPBP at 1 wt% MWCNTs–POAMA addition.

3.4. Through-plane conductivity of metal mesh–MWCNTs–POAMA/vinyl ester composite bipolar plates

Fig. 6 shows the through-plane conductivity of the original polymer composite bipolar plate, Cu-HPBP, and Al-HPBP with 1 wt% MWCNT content. The through-plane conductivity for the original polymer composite bipolar plate is significantly lower than the in-plane conductivity. This is because the graphite particles are oriented in a plane perpendicular to the direction of the compression force [41]. Thus, only few conducting paths formed in the through-plane direction lead to lower through-plane conductivity. The bipolar plates prepared with different metal meshes show through-plane conductivities of $\sigma_{original} = 37.8\ S\ cm^{-1}$ for the original polymer composite bipolar plate, $\sigma_{Cu\text{-}HPBP} = 36.7\ S\ cm^{-1}$ for Cu-HPBP, and $\sigma_{Al\text{-}HPBP} = 22.9\ S\ cm^{-1}$ for Al-HPBP. This result indicates that the through-plane conductivity of Cu-HPBP is almost the

same as the original polymer composite bipolar plate. In contrast to Cu-HPBP, the Al-HPBP exhibits relatively lower through-plane conductivity (only ~60% of the original polymer composite bipolar plate). This may be due to very high ohmic resistance of the passivation layer on the aluminum surface [42–44], although aluminum shows high corrosion resistance due to its excellent passive layer mainly composed of aluminum oxide. However, the passive layer reduces interfacial electrical conductivity between the metal mesh and polymer composite materials leading to decreased through-plane conductivity in Al-HPBP.

3.5. Single cell performances of metal mesh–MWCNTs–POAMA/vinyl ester composite bipolar plates

Fig. 7 presents polarization curve results of the five individual tests of single cells compressively assembled with the original polymer composite bipolar plate, Cu-HPBP, and Al-HPBP with 1 wt% of MWCNTs–POAMA. The open circuit voltages (OCV) of all single cell tests are the same at ~1.0 V. The current densities at 0.6 V are 0.485, 0.470 and 0.333 A cm^{-2}, and the corresponding power densities are 0.289, 0.281 and 0.199 W cm^{-2}, respectively. When introducing a metal mesh into the original polymer composite bipolar plates, the polarization curves become more identical compared to the original one, especially Cu-HPBP. Introducing metal meshes also causes decreased power density, especially Al-HPBP; however, Cu-HPBP only had a slight power density loss. The reason can be explained as follows: (1) when the metals are imbedded into the polymer composite bipolar plate, they exhibit intrinsic electrical conductivity, and may play a role similar to "current rectifier". Some graphite powders in the polymer composite bipolar plate are separated by the thin insulting polymer layers, although incorporating MWCNTs–POAMA may reduce this effect by formatting a 3-D percolating network for electrical conduction. Hence, electrons passing through the bipolar plate will probably choose the percolation conductive path to reduce electrical impedance. By contrast, the embedded metal meshes always have lowest electrical resistance; hence, the metal meshes will collect the electrons and draw them out. Copper possesses higher electrical conductivity than aluminum, and thus, its performance is more stable than aluminum; (2) the polarization curve at the median current density region is linear, so-called the "ohmic overpotential" region [40,45]. Over this region, the polarization curve is controlled by the ohmic resistance of each component. Therefore, the total resistances of single cells assembled with each composite bipolar plate (denoted as $R^0_{\text{orig.}}$, $R^0_{\text{Cu-HPBP}}$, and $R^0_{\text{Al-HPBP}}$) can be simply calculated by using ohm's law ($R^0 = P^0/(I^0)^2$) at 0.6 V. Table 2 summarizes the corresponding resistance values as 1.23, 1.27, 1.79 Ω cm^2, respectively. Compared to the original composite bipolar plates, possibly the added resistance is due to interfacial resistance between composite materials and the metal mesh. Therefore, the interfacial resistances of Cu-HPBP and Al-HPBP, denoted as $R^{\text{inter}}_{\text{Cu-HPBP}}$ and $R^{\text{inter}}_{\text{Al-HPBP}}$, are obtained by subtracting the resistance of the original polymer composite bipolar plate as the baseline resistance (ex. $R^{\text{inter}}_{\text{Cu-HPBP}} = R^0_{\text{Cu-HPBP}} - R^0_{\text{orig.}}$). The values of $R^{\text{inter}}_{\text{Cu-HPBP}}$ and $R^{\text{inter}}_{\text{Al-HPBP}}$ are 0.043 and 0.566 Ω cm^2. This result indicates that the single cell performance of Cu-HPBP is almost the same as the original polymer composite bipolar plate. In contrast to Cu-HPBP, the interfacial resistance of Al-HPBP is much higher than that of Cu-HPBP by a factor of 13. As mentioned in Section 3.4, the passive layer decreases surface electrical conductivity of aluminum leading to an obvious through-plane conductivity drop and higher interfacial resistance. Nevertheless, higher resistance may indicate that the interfacial contact resistance between metal mesh and polymer composite bipolar plate causes additional power density loss in fuel cells. However, due to the superior electrical conductivity of copper, the interfacial resistance can almost be ignored.

Table 2
Experimental data of current density, power density, total resistance, and interfacial resistance of original polymer composite, Cu-HPBP, and Al-HPBP.

Bipolar plate	Original	Cu-HPBP	Al-HPBP
Current density (A cm^{-2}) at 0.6 V, I^0	0.485	0.470	0.333
Power density (W cm^{-2}) at 0.6 V, P^0	0.289	0.281	0.199
Total resistance (Ω cm^2), R^0	1.23	1.27	1.79
Interfacial resistance (Ω cm^2), R^{inter}	–	0.043	0.566

From thermal conductivity, through-plane conductivity and cell performance data, the Cu-HPBP developed in this study exhibits higher thermal conductivity and more stable performance than that of Al-HPBP. Additionally, Cu-HPBP has almost no loss of output power density compared to the original polymer composite bipolar plate. This novel design concept of the bipolar plate may be a new category for alternative bipolar plate materials for replacing the high cost of machining graphite.

4. Conclusions

Using the chemical bonding method, this study grafts linear POAMA molecules on the MWCNT surface. The dispersion of MWCNT in the vinyl ester matrix and in-plane electrical conductivity of the bipolar plate increased due to the surface modification of MWCNTs. With functionalized MWCNTs, the current work evaluated bulk thermal conductivity and single cell performance of polymer composite bipolar plates by introducing metal mesh at the center of the bipolar plate. Results indicate enhanced bulk thermal conductivity of copper/aluminum mesh hybrid polymer composite bipolar plates from 27.2 W m^{-1} K^{-1} to 30.0 W m^{-1} K^{-1} and 30.4 W m^{-1} K^{-1}, with 10.2% and 11.7% enhancement, respectively. The through-plane conductivity of copper mesh hybrid polymer composite bipolar plate (36.7 S cm^{-1}) shows no large difference with original m-MWCNTs/polymer composite bipolar plate (37.8 S cm^{-1}). However, the aluminum mesh hybrid polymer composite bipolar plate (22.9 S cm^{-1}) exhibits an obvious decrease in through-plane conductivity due to the passivation layer on the aluminum surface. Moreover, the single cell performance observed through polarization curves provided additional information. Cu-HPBP and Al-HPBP provide higher stability than the original polymer composite bipolar plate. However, Al-HPBP showed an obvious decrease in power density due to very high ohmic resistance of the passivation layer on the aluminum surface. Therefore, the copper mesh hybrid polymer composite bipolar plate, Cu-HPBP, exhibits higher efficiency in bulk thermal conductivity enhancement and performance stability. Cu-HPBP can be utilized for high heat radiation and high stability of bipolar plates that are important for PEMFC heat management and power supplementation.

Acknowledgements

The authors are grateful to the Fuel Cell Center, Yuan Ze University, Taiwan, and Plastics Industry Development Center, Taiwan, for financial and technological supports.

References

[1] S.H. Liao, C.H. Hung, C.C.M. Ma, C.Y. Yen, Y.F. Lin, C.C. Weng, J. Power Sources 176 (2008) 175.
[2] B.D. Cunningham, J. Huang, D.G. Baird, J. Power Sources 165 (2007) 764.
[3] S.H. Liao, C.Y. Yen, C.C. Weng, Y.F. Lin, C.C.M. Ma, C.H. Yang, M.C. Tsai, M.Y. Yen, M.C. Hsiao, S.J. Lee, X.F. Xie, Y.F. Hsiao, J. Power Sources 185 (2008) 1225.
[4] G.O. Mepsted, J.M. Moore, Handbook of Fuel Cells—Fundamentals, Technology and Applications, John Wiley & Sons, Ltd., New York, 2003, pp. 286–293.
[5] A.A. Kulikovsky, J. Power Sources 160 (2006) 431.
[6] T. Yang, P. Shi, J. Power Sources 175 (2008) 390.
[7] B. Cunningam, D.G. Baird, J. Mater. Chem. 16 (2006) 4385.

[8] M.S. Wilson, D.W. Busick, US Patent 6,248,467 (2001).
[9] J. Wind, L.A. Croix, S. Braeuninger, P. Hedrich, C. Heller, M. Schudy, Handbook of Fuel cells—Fundamentals, Technology and Application, John Wiley & Sons, Ltd., New York, 2003, pp. 295–307.
[10] C.Y. Bai, Y.H. Chou, C.L. Chao, S.J. Lee, M.D. Ger, J. Power Sources 183 (2008) 174.
[11] H. Tawfik, Y. Hung, D. Mahajan, J. Power Sources 163 (2007) 755.
[12] S.T.K. Hong, K.S. Weil, J. Power Sources 168 (2007) 408.
[13] US Car & Fuel Cell Partnership, Fuel cell technologies roadmap, August 2005 (available at http://www.uscar.org/commands/files_download.php?files_id=81).
[14] J.K. Kuo, C.K. Chen, J. Power Sources 162 (2006) 207.
[15] I.E. Paulauskas, M.P. Brady, H.M. Meyer III, R.A. Buchanan, L.R. Walker, Corros. Sci. 48 (2006) 3157.
[16] H.C. Kuan, C.C.M. Ma, K.H. Chen, S.M. Chen, J. Power Sources 134 (2004) 7.
[17] S.H. Liao, C.Y. Yen, C.H. Hung, C.C. Weng, M.C. Tsai, Y.F. Lin, C.C.M. Ma, C. Pan, A. Su, J. Mater. Chem. 18 (2008) 3993.
[18] M. Wu, S.L. Leon, J. Power Sources 136 (2004) 37.
[19] L.D. Andrew, J. Power Sources 156 (2006) 128.
[20] R.C. Emanuelson, W.L. Luoma, W.A. Taylor, US Patent 4,301,222 (1981).
[21] B.B. Fitts, V.R. Landi, S.K. Roy, US Patent 6,911,917 (2004).
[22] G.W. Yeager, M. Cavazos, H. Guo, G.D. Merfeld, J. Rude, E.O. Teutsch, K.P. Zarnoch, US Patent 6,905,637 (2005).
[23] C.C.M. Ma, K.H. Chen, H.C. Kuan, S.M. Chen, M.H. Tasi, Y.Y. Yen, F.H. Tsau, US Patent 7,090,793 (2006).
[24] S. Li, Y.J. Qin, Z. Shi, X. Guo, Y. Li, D. Zhu, Chem. Mater. 17 (2005) 130.
[25] R.H. Baughman, A.A. Zakhidov, W.A. de Heer, Science 297 (2002) 787.
[26] R. Haggenmueller, J. Chen, H.Y. Liu, Appl. Phys. Lett. 83 (2003) 2928.
[27] C.H. Tseng, C.C. Wang, C.Y. Chen, Chem. Mater. 19 (2007) 308.
[28] D. Stauffer, A. Aharnoy, Introduction to Percolation Theory, Taylor & Francis, London, 1991.
[29] S. Kitta, H. Uchda, M. Watanabe, Electrochim. Acta 3 (2007) 2025.
[30] J. Zhu, H. Peng, F. Rodriguez-Macias, J.L. Margrave, V.N. Khabashesku, A.M. Imam, K. Lozano, E.V. Barrera, Adv. Funct. Mater. 14 (2004) 643.
[31] Y. Lin, A.M. Rao, B. Sadanadan, E.A. Kenik, Y.P. Sun, J. Phys. Chem. B 106 (2002) 1294.
[32] Y. Zhang, A.A. Broekhuis, M.C.A. Stuart, T.F. Landaluce, D. Fausti, P. Rudolf, F. Picchioni, Macromolecules 41 (2008) 6141.
[33] Y. He, Thermochim. Acta 436 (2005) 122.
[34] M. Gustavsson, E. Karawacki, S.E. Gustafsson, Rev. Sci. Instrum. 65 (1994) 3856.
[35] T. Log, S.E. Gustafsson, Fire Mater. 19 (1995) 43.
[36] V. Bohac, M.K. Gustavsson, L. Kubicar, S.E. Gustafsson, Rev. Sci. Instrum. 71 (2000) 2452.
[37] Hot Disk Thermal Constants Analyser Instruction Manual, Mathis Instruments, Fredericton, New Brunswick, Canada, 2001.
[38] National Physical Laboratory, Transient Plane Source—Gustafsson Hot Disk Technique, Standards for Contact Transient-Measurements of Thermal Properties, National Physical Laboratory, United Kingdom. http://www.npl.co.uk/thermal/ctm (accessed May 2006).
[39] C.Y. Yen, S.H. Liao, Y.F. Lin, C.H. Hung, Y.Y. Lin, C.C.M. Ma, J. Power Sources 162 (2006) 309.
[40] A. Faghri, Z. Guo, Int. J. Heat Mass Transf. 48 (2005) 3891.
[41] J. Huang, D.G. Baird, J.E. McGrath, J. Power Sources 150 (2005) 110.
[42] J.K. Neutzler, US Patent 5,776,624 (1998).
[43] J. Wind, R. Späh, W. Kaiser, G. Böhm, J. Power Sources 105 (2002) 256.
[44] V. Mehta, J.S. Cooper, J. Power Sources 114 (2003) 32.
[45] D. Chu, R. Jiang, J. Power Sources 80 (1999) 226.